Annealing effects on the mass diffusion of the CdS/ITO interface deposited by chemical bath deposition

A. Ordaz-Flores*, P. Bartolo-Pérez**, R. Castro-Rodríguez, and A.I. Oliva*
Departamento de Física Aplicada, Centro de Investigación y de Estudios Avanzados del IPN,
Apartado Postal 73 Cordemex, 97310 Mérida, Yucatán, México,
e-mail: oliva@mda.cinvestav.mx

Cadmium sulphide thin films prepared by chemical bath deposition (CBD) were deposited on indium tin oxide (ITO) substrates with different deposition times (*i.e.* thickness) and characterised by their morphology and band gap energy. Samples were analysed as deposited and after annealing at 90 and 150°C, in order to study the interface diffusion and its effects on the properties mentioned. Auger depth profiles were used to determine the mass diffusivity coefficient in the CdS/ITO interface. The initial surface rms-roughness measured with AFM, as well as the initial band gap energy, are reduced after the annealing process. We obtained very small diffusion coefficient values, around 10^{-21} m^2/s, for the different elements analysed in the interface.

Keywords: CdS/ITO interface; CBD; CdS films; ITO substrate; mass diffusion.

Capas delgadas de sulfuro de cadmio, preparadas por baño químico, fueron depositadas sobre sustratos de ITO (óxido de estaño impurificado con indio) con diferentes tiempos de depósito (*i.e.* espesor) y caracterizadas en su morfología y en su brecha de energía. Las muestras fueron analizadas tanto recién depositadas como después de ser recocidas a las temperaturas de 90 y 150°C, con el objetivo de estudiar la difusión en la interfaz CdS/ITO y sus efectos sobre las propiedades mencionadas. Con ayuda de los perfiles Auger, se determinaron los valores de la difusividad másica de dicha interfaz. El valor inicial rms de la rugosidad superficial medida usando imágenes de fuerza atómica, así como la brecha de energía, se ven reducidos después de los procesos de recocido. Se obtuvieron valores muy pequeños en los coeficientes de difusión, del orden de 10^{-21} m^2/s, para los diferentes elementos analizados en la interfaz.

Descriptores: Interfaz CdS/ITO; baño químico; películas delgadas de CdS; substrato ITO; difusión de masa.

PACS: 68.55.Nq; 79.60.Jv; 81.15.Lm; 82.80.Pv

1. Introduction

The technology for the promising high efficient CdS/CdTe solar cells requires a conductor substrate for improving. For this junction about 16% solar conversion efficiency has been demonstrated in the laboratory [1]. Indium tin oxide (ITO) films are usually deposited on glass substrate in order to control their thickness and consequently their electrical conductivity. Normally, ITO is used both as a conductor and as an electrode to support the CdS thin film into the heterostructure CdTe/CdS/ITO/glass solar cell [2]. An interesting interface is formed when CdS is deposited by CBD technique on ITO substrate [3], which quality is related to the efficiency of the prepared solar cells. The interfaces qualities play an important role in facilitating the free electron flow through the complete solar cell to obtain high efficiency. Controlled changes in the properties of this interface can produce variations in the conductive properties of the semiconductor. Several efforts toward to study CdS/ITO [4, 5] and the CdS/CdTe [6] interfaces have been reported in the literature. Some published works predict the importance of the interface quality and the interdiffusion mechanisms related to it. Annealing processes are normally made as attempts to reduce the intrinsic stress improving the lattice mismatch and to produce longer trajectories for the free electrons for better electrical conductivity. The knowledge of the most appropriate temperature for depositing the CdS onto the ITO substrates and the optimal an-

nealing process would make it possible to control the formed interface, in order to improve the lattice mismatch and to increase the efficiency of the solar cell. The CBD technique has proven to be an ideal technique to produce uniform and very thin films with low cost and simplicity. Films produced with this technique are convenient to allow a good electric conductivity and enough thickness such that the CdS material does not disappear when mixed with substrate in the interface (in our case, ITO).

2. Theory

In order to calculate the diffusion coefficient *D*, we choose the linear semi-infinite diffusion model, by the geometry of the formed interface, and we take the results obtained from a depth profile concentration determined by the Auger electron spectroscopy (AES) technique. This is valid for the thin-film configuration if we assumed that we can obtain accurate concentration data at very short times [7]. For that, we need to solve the temporal and one-dimensional Fick's second law of diffusion given by:

$$\frac{\partial C(x,t)}{\partial t} = D \frac{\partial^2 C(x,t)}{\partial^2 x^2} \tag{1}$$

for the initial conditions $c(x,0)=0$ and $c(0,t)=c_0$, and which solution is given by

$$\frac{c}{c_0} = \text{erfc}\left(\frac{x}{2\sqrt{Dt}}\right) \qquad (2)$$

where *erfc(z)* is the complimentary error function, *x* the depth of an element from the interface, *t* the deposition time, *D* the diffusion coefficient and $z = x/(2\sqrt{Dt})$. Values of *z* are tabulated for *x*, so by defining

$$m = \frac{1}{2\sqrt{Dt}} \qquad (3)$$

and rewriting the solution (1) as $c/c_0 = \text{erfc}(mx)$, we can find the corresponding linear regression to calculate the slope *m*, by means of which we can calculate the diffusion coefficient *D*. The concentration profile c/c_0 as a thickness (or time) function for a certain element is obtained from the Auger profile.

3. Experimental details

CdS thin films were deposited on 1×1 cm^2 ITO substrates cleaned with soap, acetone and isopropyl alcohol and rinsed with distilled water between each step. CdS films were prepared by CBD technique with magnetic agitation. Details of the technique are widely described in the literature [8, 9]. Briefly, the total volume (110 ml) of the chemical bath is formed by an aqueous solution containing the following molar concentrations of each reactant: 0.02 M cadmium chloride (CdCl$_2$), 0.5 M potassium hydroxide (KOH), 1.5 M ammonium nitrate (NH$_4$NO$_3$), and 0.2 M thiourea (CS[NH$_2$]$_2$) as a catalytic reagent. This is a widely used recipe for obtaining good quality films [10]. The bath temperature was controlled at $75 \pm 1°$C by means of a Teflon covered type K thermocouple and connected to a home-made temperature controller, based on a CN4421TR-D1 Omega device with a solid state relay. This temperature is widely used to obtain the CdS compound from the chemical components in order to achieve a reasonable deposition rate. A lower bath temperature retards the CdS deposition rate, and a higher temperature produces a higher evaporation of the chemical bath and an uncontrollable deposition rate. The ITO substrates were supported by Teflon holders when they were immersed in the chemical bath. Film deposition starts when thiourea is added. Each sample holder and deposited film is retired one by one from the bath after 10, 20, 30, 40, and 50 minutes of deposition time. The resulting transparent and pale yellow films present bright surfaces and high adherence to the substrates, so that to eliminate the CdS film from one face of the substrate (for optical measurements) we need to use an HCl solution. The chemical bath solution was agitated with a magnetic stirrer during deposition. This method, used to produce high-quality CdS films, is very useful for avoiding concentration gradients of the bath or colloids [8].

Annealing processes were carried out under clean conditions in a Fischer Scientific Vacuum Oven model 280, at 635 Torr. Annealing temperatures were measured with a mercury thermometer. All films were annealed for three hours at two temperatures: 90° and 150°C. These conditions were chosen as representative to produce clear diffusion in the CdS/ITO interface and higher than the chemical bath temperature during deposition. Optical and surface measurements were made after films deposition and after each annealing process.

AFM images of films surfaces were obtained in the constant force mode with a high-resolution scanner (5×5 μm^2). The mean rms-roughness values for three images of different sites of each film were obtained at atmospheric pressure and room temperature and an average value is reported for statistics.

Film thickness was estimated from compositional depth profiles performed by the Auger technique, with an ESCA/SAM Perkin Elmer PHI 560 equipment yielding a sputtering rate of about 10 nm/min with Ar$^+$ ions. The CdS film thickness was determined as the point where the Cd and S signals from the film mix with the Sn and In signals coming from the ITO substrate. Thus, by knowing the sputtering time of the depth profiles, the CdS film thickness can be deduced. This technique was also used to measure at the same time, the concentration of elements in the CdS/ITO interface while it is bombarding with Argon ions. Optical absorption measurements were taken with a Jobin-Yvon/Spex H20-VIS spectrophotometer using a 250 W tungsten halogen lamp, with normal flux to the film surface. The wavelength was ranged from 300 to 800 nm. The resulting signal was received and processed with a Data Scan-2 controller coupled to a computer. Optical analysis were made after eliminating the effect of the ITO/glass substrate from the deposited CdS/ITO/glass film. From here, we determined the CdS direct band gap energy (E$_g$) of CdS films by using the relation

$$\alpha^2 = \frac{1}{d^2}\ln^2\left[\frac{I_0}{I}\right] = A(E - E_g), \qquad (4)$$

with α being the absorption coefficient, *d* the film thickness, *I* and I_o the transmitted and emitted light intensities, respectively, *C* a constant, and *E* the light energy.

4. Results and discussion

4.1. As-deposited films

The rms-roughness and the estimated thickness values of the as-deposited CdS films are shown in Table I. Film thickness uncertainties are due to the standard deviations obtained from four profiles made on different sites of the sample. Values of the rms-roughness do not show an ordered behaviour with time deposition maybe by the initial high ITO rms-roughness (15 nm); however, the lower values obtained in the reported values indicates flatness films surfaces. The band gap energies measured for the CdS/ITO samples are also included in Table I. The reported E$_g$ values are measured with a 0.01 eV of uncertainty as estimated from the light intensity detector

and the monochromator device resolution. The highest value of the band gap energy obtained for the thinnest film ($\sim$ 8 nm for 10 min as deposition time) is in good agreement with the quantum confinement effect of the electrons expected for this thickness range [11]. Similar behaviour has been reported for our group during the formation of the band gap of the CdS films [12] during the first stage of growth. Values of the band gap reported for the thickest films correspond to the direct band gap values of polycrystalline films measured at room temperature ($2.42 - 2.45$ eV). X-ray diffraction analysis show that CdS films present a cubic structure with a strong orientation in the (111) reflection peak and minor orientations in the (220) and (311) peaks.

During the Auger depth profile analysis, we measured the concentration of the Cd and S elements from the CdS film, and Sn and In from the ITO substrate. Oxygen from ITO was not recorded during the analysis because we considered that it was not important in this study.

From these data, we calculated the diffusion coefficient of these elements for the different samples by means of Eq. (3). We used a 10 nm/min value as erosion rate during Ar^+ ions as calibrated for SiO_2/glass standard film. Values of these coefficients are shown in Fig. 1 for the as-deposited CdS films. The calculated diffusion coefficients vary in the 10^{-21}-10^{-22} m^2/s range, small values compared with high temperature processes [12]. Thicker CdS films show slightly higher values on the diffusion coefficient. From Fig. 1, two diffusion slopes can be assumed: a rapid diffusion observable during the first stages of growth, and a slower one as the deposition time increases (*i.e.*, thickness increases). However, it is not an easy task to identify the associated diffusion mechanism. Given that the S atom has a smaller atomic radius than Sn, Cd and In atoms, is probably than it interstitially diffuses into the interface, but we do not know enough about the vacancies or defects in the crystallographic structure or the grain size and grain boundaries. More detailed work needs to be done in order to understand the diffusion mechanism.

4.2. Annealed films

Annealing is a common process used for reducing stress on deposited films, to improve mismatch, and to achieve interdiffusion between elements through an interface. As-deposited films were annealed at two different temperatures: 90 and 150°C, two temperatures above the chemical bath temperature and for three hours, enough time to reduce me-

TABLE I. Characteristics of the CdS film as-deposited on ITO substrates by CBD at 75°C.

Sample	Deposition time (min)	Thickness (nm)	Rms-roughness value (nm)	Band gap energy (eV)
1	10	7.5 ± 0.8	11.2	2.52
2	20	8.9 ± 0.6	13.6	2.46
3	30	11.9 ± 0.4	11.5	2.44
4	40	13.3 ± 0.4	11.5	2.45
5	50	13.7 ± 0.4	14.6	2.44

TABLE II. Diffusion coefficients (m^2/s) calculated after a 90°C annealing process on the CdS/ITO interface from Auger depth profile.

Sample	S($\times 10^{-22}$)	Cd($\times 10^{-22}$)	Sn($\times 10^{-22}$)	In($\times 10^{-22}$)
1	1.65	1.62	1.42	0.869
2	4.23	3.00	2.49	1.83
3	34.9	7.84	13.9	9.65
4	2.43	1.75	1.53	1.17
5	24.8	7.84	7.10	5.76

TABLE III. Diffusion coefficients (m^2/s) calculated after a 150°C annealing process on the CdS/ITO interface from Auger depth profile.

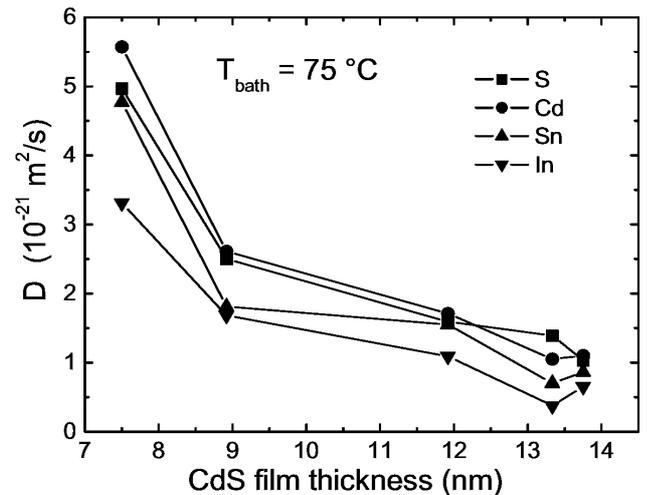| Sample	S($\times 10^{-21}$)	Cd($\times 10^{-21}$)	Sn($\times 10^{-21}$)	In($\times 10^{-21}$)
1	0.155	0.119	0.145	0.0869
2	7.47	7.54	6.06	4.46
3	2.59	2.69	2.73	2.09
4	6.03	6.44	5.35	4.12
5	4.36	4.53	3.32	2.50

FIGURE 1. Estimated diffusivities values as a function of the CdS film thickness obtained for the as-deposited CdS/ITO interface.

chanical stress and to induce mass diffusion at the interface. After each annealing, the surface morphology, the band gap energy and the diffusion coefficient were obtained.

Figure 2 shows AFM images of the evolution of the surface morphology of sample 2, according to the annealing processes. A rearrangement of the grains, becoming larger and flatter, with the increase of the temperature, mainly after the 150°C annealing process, was observed. Similar behaviour was observed in the other film thicknesses.
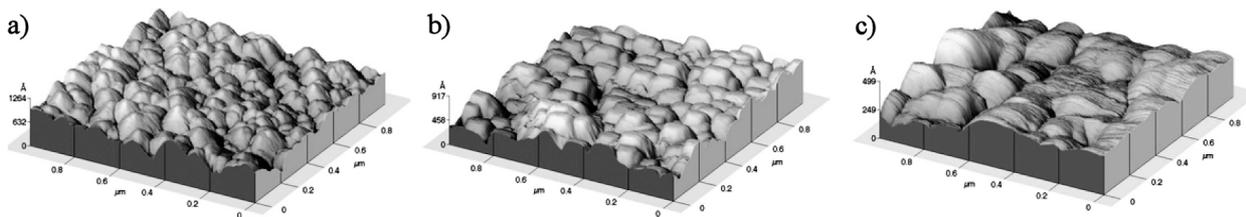
FIGURE 2. AFM images (1×1 μm^2) of CdS thin films grown on ITO/glass deposited by CBD at 75°C during 20 min; (a) as deposited, (b) after annealing at 90°C, and (c) after annealing at 150°C.
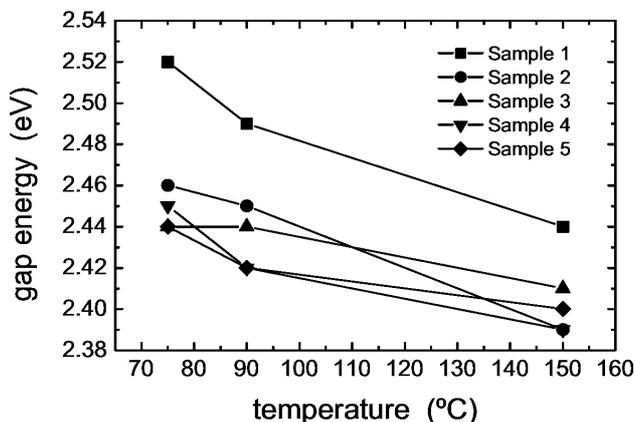

FIGURE 3. Behaviour of the band gap energy values with temperature. Corresponding temperatures are: deposition, 75°C; first annealing process (90°C) and second annealing process (150°C). Film thickness increases with the ample number according with Table I.
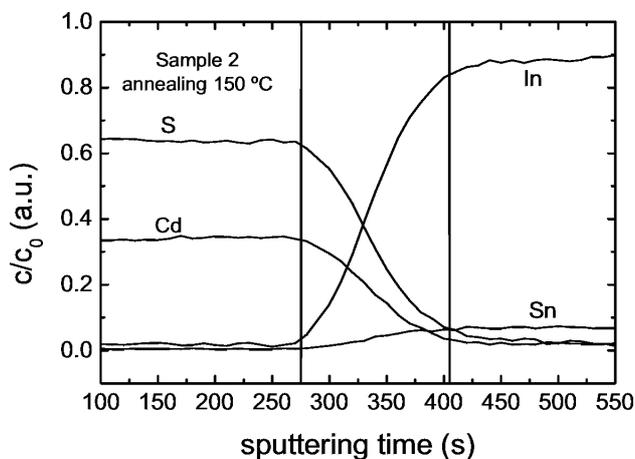

FIGURE 4. Concentration depth profile of the CdS/ITO interface of sample 2 after annealing at 150°C. The interface is marked between vertical lines.
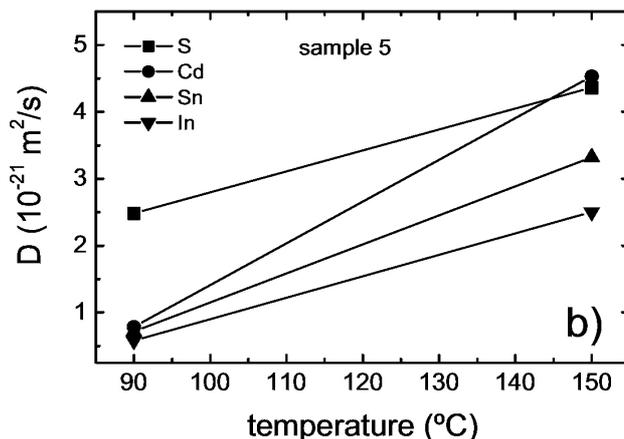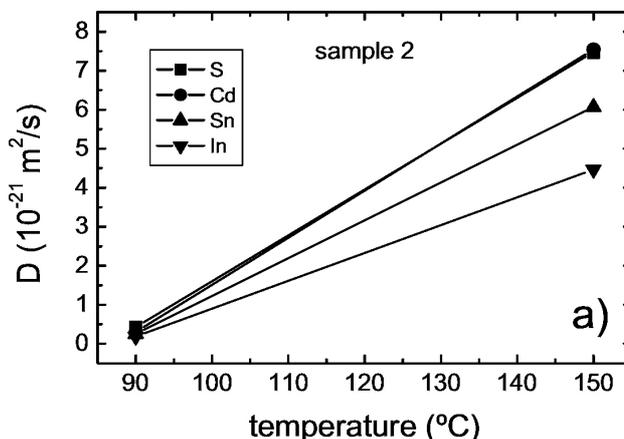

FIGURE 5. Changes of the diffusivity values after from annealing process at 90 and 150°C on the CdS/ITO interface. Film deposition time. (a) sample 2 (20 min); (b) sample 5 (50 min).

The optical band gap energy of each film thickness were measured as-deposited and after each annealing process. Figure 3 shows the results. Higher annealing temperatures cause a decrement in the band gap energy value in all films. Presumably, during the annealing process, atoms rearrange to more energetic and suitable positions on the valence band. In this way, the photo-current can be increased by the longer mean free path of electrons, so that less energy is needed for an electron to jump to the conduction band.

Rms-roughness values show an almost constant behaviour on film surface before and after the annealing processes, with no tendencies to increase or diminish in any case. As can be deduced from the AFM images, the annealing process is not a parameter that could affect the surface rms-roughness value behaviour in this thickness range. However, grain size on the film surface is observed clearly to increase with the annealing treatment. According to the literature, minor grain size produces a larger diffusion velocity because of the larger space between grains if the diffusion is produced by grain boundaries.

Auger depth profiles are normally used for chemical analysis. We used this technique for film thickness determination,

given the small thickness produced by the small deposition time. Film thickness proved difficult to calculate with this technique after annealing, because of the larger grain size; for that reason, the thickness value considered in this work as reference for further calculations is the value measured for the as-deposited films. Figure 4 shows a typical Auger depth profile obtained for the CdS/ITO interface. Profiles of the main elements mixed in the interface are monitored. Concentration profiles obtained for the Auger technique correspond also for sample 2, but similar behaviour was obtained for the other film thickness. From these profiles, and using the equations discussed in Sec. 2, we calculated the diffusion coefficient D for each element after each annealing process.

Diffusion coefficient values calculated for the different elements involved on the CdS/ITO interface were found to range between 10^{-21} and 10^{-22} m^2/s after the first annealing process at 90°C was completed. A slower diffusion process is observed as compared with the as-deposited films, so that we believe that a different diffusion mechanism could be involved. The annealing process causes the movement of atoms because of the originated rearrangements so that grain boundary diffusion and interstitial diffusion could the most probable processes involved. In all cases, the S stands out to be more easily diffusible than the other elements by the higher values calculated in all cases (see Table II).

An important point to regard is that the deposited film during 10 min, presents the lowest diffusion coefficients in all cases. Given that is the thinnest thickness (8 nm), it has less material to diffuse, as compared with the thickest films, the crystalline structure is forming yet and quantum effects can be given.

After the second annealing process at 150°C (Table III), the diffusion rates are, in general, faster than the first annealing. This can be better seen from the plots shown in Fig. 5. Grain boundary and interstitially diffusion can be the most appropriate diffusion mechanism after this process. However, the effect of second annealing process was higher diffusion coefficients and a wider interface. Contrarily to the first annealing, the wideness of the interface changed considerably after the 150°C annealing process. The annealing at 90°C does not seem to make interesting changes in the morphology nor the diffusion coefficients, but it is enough to appreciate changes in the band gap. Then, high annealing temperatures stand out to be performed in further studies focused on diffusivity and morphology.

Dispersion on the diffusivity values described on Tables II and III, are due to the surface roughness condition of the analysed samples. By the local characteristic of the Auger technique, the depth profile analysis will depend on the site when the beam hits. Given that film roughness changes with annealing temperature, then, depth profile can change from site to site on sample, and consequently, the detected elements (S, Cd, In, and Sn) can vary on concentration. However, the implemented method to calculate the coefficient of diffusivity can be useful to study and quantify diffusion on the interfaces of bimaterial layers.

Acknowledgments

∗ Tesista de Ingeniería Física de la Facultad de Ingeniería de la UADY.

∗∗ On leave on the Programa de Corrosión del Golfo de México de la UAC.

1. J. Britt and C. Ferekides, *Appl. Phys. Lett.* **62** (2001) 2851.

2. Dieter Bonnet, *Cadmium telluride solar cells*. In *Clean electricity from photovoltaics*, Mary D. Archer y Robert Hill, (Editors). (Imperial College Press, London, 2001).

3. A.I. Oliva *et al.*, *Appl. Surf. Sci.* **148** (1999) 42.

4. A. Martel *et al.*, *Phys. Stat. Sol. b* **220** (2000) 261.

5. K.D. Dobson, I. Visoly-Fisher, G. Hodes, and D. Cahen, *Sol. Energy Mat. & Sol. Cells* **62** (2000) 295.

6. B.E. McCandeless, M.G. Engelmann, and R.W. Brikmire, *J. Appl. Phys.* **89** (2001) 988.

7. M.E. Glicksman, *Diffusion in Solids* (John Wiley & Sons. 2000) Chapter 3, p. 472.

8. J.M. Doña and J. Herrero, *J. Electrochem. Soc.* **144** (1997) 4081.

9. D. Lincot and R. Ortega-Borges, *J. Electrochem. Soc.* **140** (1993) 3464.

10. J.M. Doña and J. Herrero, *J. Electrochem. Soc.* **144** (1997) 4091.

11. K.K. Nanda, S.N. Sarangui, S. Mohantay, and S.N. Sahu. *Thin Solid Films* **322** (1998) 21.

12. A.I. Oliva, O. Solís, R. Castro-Rodríguez, and P. Quintana, *Thin Solid Films* **391** (2001) 28.